Geophysical Research Letters

RESEARCH LETTER
10.1029/2021GL097198

Reconciling Roles of External Forcing and Internal Variability in Indian Ocean Decadal Variability Since 1920

Wenjian Hua[1], **Aiguo Dai**[2], **and Minhua Qin**[3]

[1]Key Laboratory of Meteorological Disaster, Ministry of Education (KLME)/Joint International Research Laboratory of Climate and Environment Change (ILCEC)/Collaborative Innovation Center on Forecast and Evaluation of Meteorological Disasters (CIC-FEMD), Nanjing University of Information Science and Technology, Nanjing, China, [2]Department of Atmospheric and Environmental Sciences, University at Albany, State University of New York, Albany, NY, USA, [3]Department of Atmospheric and Oceanic Sciences and Institute of Atmospheric Sciences, Fudan University, Shanghai, China

Abstract On decadal time scales, Indian Ocean sea surface temperatures (SSTs) exhibit coherent basin-wide changes, but their origins are not well understood. Here we analyze observations and model simulations from Coupled Model Intercomparison Project Phase 6 and Community Earth System Model Version 1 to quantify the roles of external forcing and internal climate variability in causing Indian Ocean decadal SST variations. Results show that both external forcing and internal variability since 1920 have contributed to the observed decadal variations in linearly detrended Indian Ocean SSTs, and they exhibit an out-of-phase relationship since the 1950s. The internally-generated variations arise from remote influences from the tropical Pacific and possible contributions from internal local processes, while the influence from the Atlantic Multidecadal Oscillation is opposite to that of the Interdecadal Pacific Oscillation. Decadal SST changes caused by nonlinear variations in greenhouse gases and aerosols are roughly out-of-phase with the internal variability, thus dampening observed SST variations since the 1950s.

Plain Language Summary Decadal variations in Indo-Pacific Ocean sea surface temperatures under global warming have received considerable attention. Indian Ocean decadal variability has been considered as a remote response to the Pacific decadal variability, despite that external forcing may also play a significant role. By analyzing observations and Coupled Model Intercomparison Project Phase 6 and Community Earth System Model Version 1 model simulations, we show that both external forcing and internal variability have caused decadal SST variations during 1920–2020 in the Indian Ocean. Internal climate variability arises from not only remote influences from the tropical Pacific and North Atlantic oceans, but also local processes. Our results also suggest that decadal variations in external forcing (i.e., greenhouse gases and anthropogenic and volcanic aerosols) dampened observed decadal variations since the 1950s.

Key Points:

- Both external forcing and internal climate variability have regulated the observed decadal Indian Ocean Basin Mode (IOBM) variations since 1920
- Internal decadal IOBM variations since 1920 arise from the tropical Pacific and North Atlantic oceans
- Decadal Ocean sea surface temperature variations in response to aerosol forcing are roughly out-of-phase with the internal decadal IOBM since the 1950s

Supporting Information:

Supporting Information may be found in the online version of this article.

Correspondence to:

A. Dai and M. Qin,
adai@albany.edu;
qinminhua@gmail.com

Citation:

Hua, W., Dai, A., & Qin, M. (2022). Reconciling roles of external forcing and internal variability in Indian Ocean decadal variability since 1920. *Geophysical Research Letters*, *49*, e2021GL097198. https://doi.org/10.1029/2021GL097198

Received 8 JAN 2022
Accepted 21 APR 2022

1. Introduction

The Indian Ocean has experienced a pronounced warming trend since the early 20th century (Deser et al., 2010), which increasingly affects Indo-Pacific climate (Li et al., 2016; Luo et al., 2012; Xie et al., 2009; Zhang et al., 2019). On decadal time scales, a basin-wide warming or cooling mode dominates the variability in the Indian Ocean sea surface temperatures (SSTs) since 1900, which is referred to as the Indian Ocean basin mode (IOBM) (Han, Meehl et al., 2014; Han, Vialard et al., 2014). Decadal variations of the Indian Ocean basin mode (IOBM) have significant impacts on regional (e.g., East Asian) and global climate (Cai et al., 2019; Han, Vialard et al., 2014; Luo et al., 2012); thus, improved understanding of the decadal Indian Ocean basin mode (IOBM) variations is of great importance for future climate prediction.

The prevailing view is that decadal IOBM variations are a response to remote forcing from the Interdecadal Pacific Oscillation (IPO) (Dong et al., 2016; Han, Meehl et al., 2014; Han, Vialard et al., 2014), whose variations have resulted primarily from internal climate variability since 1920 (Hua et al., 2018). However, the relationship between the decadal variations of the IOBM and Interdecadal Pacific Oscillation (IPO) is nonstationary and has changed in recent decades (Dong & McPhaden, 2017; Han, Meehl et al., 2014; Zhang et al., 2018). Specifically, the decadal IOBM variations were positively correlated with the Interdecadal Pacific Oscillation (IPO) before the mid-1980s, but the correlation became negative afterwards (Dong & McPhaden, 2017; Han, Meehl

et al., 2014). Previous studies have attributed this change to greenhouse gas (GHG) and volcanic forcings (Dong & McPhaden, 2017; Zhang et al., 2018). However, a changed relationship also occurred in the 1960s, but it has received little attention (Dong & McPhaden, 2017). Thus, the competing effects on the decadal IOBM from external forcing (e.g., greenhouse gases (GHGs) and aerosols) and internal climate variability (e.g., IPO) during the 20th century are still not well understood. On the other hand, the remote influence from the North Atlantic Ocean may also have contributed to multidecadal SST variations in the Indian Ocean (Li et al., 2016; McGregor et al., 2014). The warming since the 1990s in the tropical and North Atlantic Ocean led to Indo-Pacific Ocean SST variations with cooling in the central Eastern Pacific and warming in the Western Pacific and Indian Ocean (Li et al., 2016). The recent warm anomaly in the North Atlantic is partly due to a warm phase of the Atlantic Multidecadal Oscillation (AMO), thus the AMO may also modulate the Indian Ocean SSTs and alter their relationship with the IPO (Cai et al., 2019; Wang, 2019). As the AMO cycles resulted from both internal climate variability and aerosol forcing (Hua et al., 2019; Qin et al., 2020a, 2020b; 2022), further research is needed to quantitatively determine the relative importance of external forcing and internal variability for the decadal SST variations in the Indian Ocean.

By analyzing observations and climate model simulations, this study aims to quantify the roles of external forcing and internal variability in the Indian Ocean decadal SST variations since 1920. Our findings should help improve current understanding of Indian Ocean decadal variability, especially its response to external forcing and internal variability.

2. Data, Model Simulations, and Methods

2.1. Observational Data and Model Simulations

We used the monthly SST data from the Hadley Centre Global Sea Ice and Sea Surface Temperature (HadISST) (Rayner et al., 2003). We analyzed the large ensemble of historical all-forcing (i.e., Community Earth System Model Version 1 Large Ensemble, CESM1-LE) and single forcing (Deser et al., 2020) simulations and an 1800 yr fully coupled preindustrial control run by the Community Earth System Model Version 1 (CESM1) model (Kay et al., 2015). We also analyzed the coupled climate model simulations from the Coupled Model Intercomparison Project Phase 6 (CMIP6) (Eyring et al., 2016; Table S1 in Supporting Information S1). See Supporting Information S1 for more information about the CESM1 and CMIP6 experiments.

We used the coupled climate model simulations from the pacemaker experiments forced by time-varying SSTs over a limited domain by CESM1 (Deser et al., 2017; Yang et al., 2020). The observed SST evolutions over the North Atlantic, tropical Pacific, or tropical Indian Ocean are maintained in each pacemaker simulation during 1920–2013, with the rest of the world being fully coupled. All external (both anthropogenic and natural) forcings are identical to the CESM1-LE, aside from stratospheric ozone (Yang et al., 2020). Note that the difference in external forcing is found to be negligible and has minimal effects on the tropical climate (Yang et al., 2020; Zhang et al., 2019). The CESM1 pacemaker ensembles simulate IPO or AMO evolution in line with observations, whereas the CESM1-LE or CMIP6 ensembles simulate their own random or realization-dependent IPO or AMO variations.

2.2. Methods

By definition, an oscillation is the deviation from the long-term mean (for stationary series) or the long-term trend (for nonstationary series) (Qin et al., 2022). Therefore, we removed the linear trend in all data series over 1920–2020 (including external forcing data) to focus on the nonlinear, decadal variations. However, such linearly-detrended variations (e.g., in observed SSTs, Dong & McPhaden, 2017; Han, Meehl et al., 2014; Zhang et al., 2018) may still include externally-forced (EX) changes from external forcing (Dai et al., 2015; Qin et al., 2020a, 2020b, 2022; Steinman et al., 2015) (Figure S1 in Supporting Information S1). To separate the EX and internally-generated (IV) components in the observations, we first used the global-mean SST from the CESM1 ensemble mean (EM) or CMIP6 multi-model ensemble mean (MMM) of the all-forcing simulations as the EX signal during 1920–2020 for EM or 1920–2014 for MMM. We then removed the changes and variations (the EX component) at each grid point associated with this forced signal from the observed SST through linear regression (Dai et al., 2015; Qin et al., 2020a), and the residual was considered as the IV component. This method

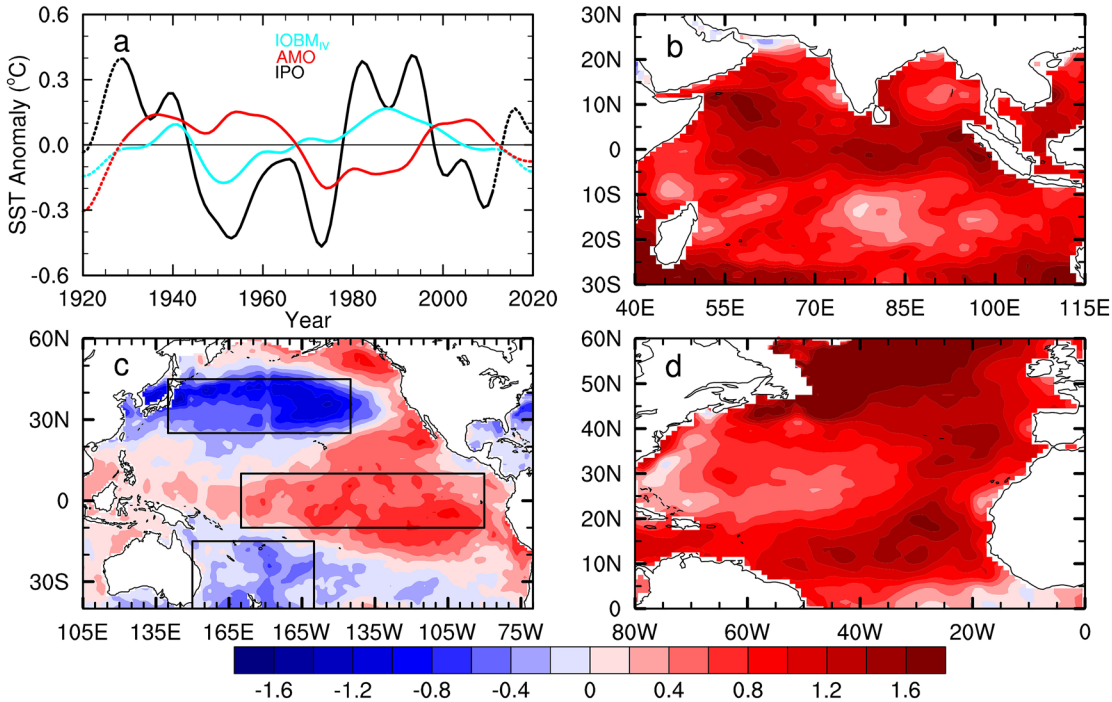

Figure 1. (a) Time series of the observed smoothed annual sea surface temperature (SST) fields (°C, with the EX component being removed) over the Indian, Pacific and North Atlantic oceans from 1920 to 2020. We used the Community Earth System Model Version 1 ensemble mean as the estimate of the forced signal and removed it from the observations to define the IV component (see methods). We defined the internally-generated decadal IOBM index (IOBM$_{IV}$, blue line) and Atlantic Multidecadal Oscillation (AMO) index (AMO$_{IV}$, red line) as the smoothed internally-generated SST anomalies averaged over the Indian (30°S–30°N, 40°–115°E) and North Atlantic (80–0°W, 0°–60°N), respectively. The Interdecadal Pacific Oscillation (IPO) index (IPO$_{IV}$, black line) is defined as the difference of the regional-mean SST anomalies between the central equatorial Pacific (10°S–10°N, 170°E–90°W) and the mean of the northwestern (25°–45°N, 140°E–145°W) and southwestern (40°–15°S, 150°E–160°W) Pacific Ocean following Henley et al. (2015). The data near the two ends (marked by dashed lines and excluded in the calculation) were derived with mirrored data in the filtering and thus are less reliable. (b–d) The pattern of the decadal IOBM$_{IV}$, IPO and AMO obtained by regressing smoothed SST anomalies from 1920 to 2020 onto the decadal IOBM$_{IV}$, IPO and AMO indices.

has been widely used in obtaining the EX and IV components in the observations (Dai & Bloecker, 2019; Dai et al., 2015; Hua et al., 2021; Qin et al., 2020a, 2020b, 2022).

We defined a total decadal IOBM index (referred to as IOBM) as the linearly detrended and smoothed SST anomalies from observations or model simulations averaged over the Indian Ocean (30°S–30°N, 40°E–115°E). The internally-generated decadal IOBM index (IOBM$_{IV}$) was defined similarly by averaging the smoothed SST anomalies resulting from internal variability over the Indian Ocean. The externally-forced IOBM index (IOBM$_{EX}$) was defined as the IOBM minus IOBM$_{IV}$ index. The results are similar when using the principal component of the leading empirical orthogonal function (EOF) mode of the linearly detrended SST fields over the Indian Ocean to represent these IOBM indices (Figures 1a and 1b and Figures S2a and S2b in Supporting Information S1). We applied a low-pass Lanczos filter to emphasize decadal to multidecadal variations (Hua et al., 2018). A correlation coefficient (r) and its significance level (p value) were calculated between two variables (e.g., decadal IOBM, AMO or IPO) to quantify their association. The significance level was estimated based on a two-sided Student's t test with an estimated effective degree of freedom to account for autocorrelation (Davis, 1976; Qin et al., 2020a).

As the 20-member Pacific pacemaker ensemble simulations share the same external forcing (as in the CESM1-LE) and tropical Eastern Pacific (TEP) SST variations, we use their EM to represent the TEP induced variations. Since the internal climate variability among the ensemble runs is uncorrelated, we use the EM of the 40-member historical runs from CESM1-LE to represent the forced change. Thus, the EM difference between the two experiments results mainly from the internally-generated TEP induced variations. Similar approaches have been applied to analyze the 10-member Atlantic and Indian pacemaker ensembles (i.e., internally-generated Atlantic-induced or Indian-induced variations).

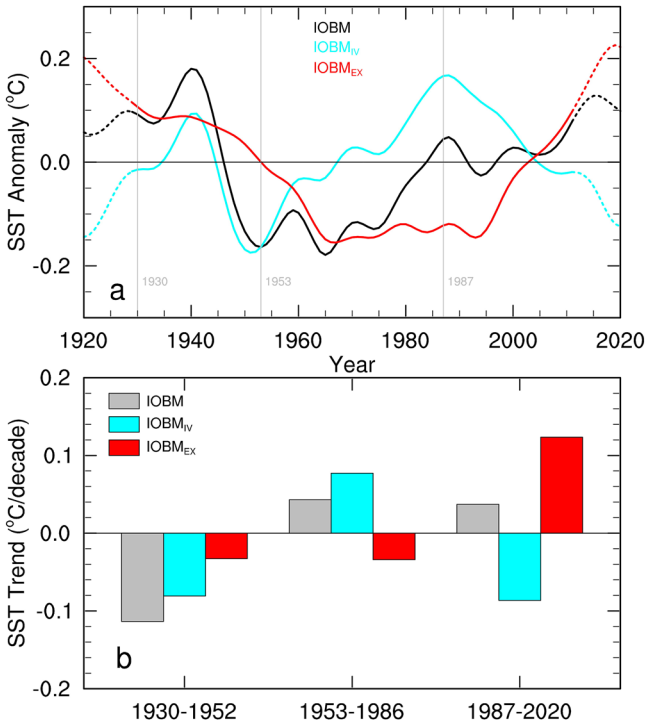

Figure 2. (a) Time series of the linearly detrended and smoothed sea surface temperature (SST) anomalies (°C) averaged over the Indian Ocean for the total decadal variations Indian Ocean basin mode (IOBM) and its internally-generated ($IOBM_{IV}$) and externally-forced ($IOBM_{EX}$) components. The $IOBM_{IV}$ is the same as the blue line in Figure 1a. (b) Indian SST linear trend (°C per decade) from observations (gray), its $IOBM_{IV}$ (blue) and $IOBM_{EX}$ (red) components for the three different periods marked by the thin vertical lines in (a).

3. Results

3.1. Internal Versus Forced Indian Decadal Variations

The $IOBM_{IV}$ (blue line in Figure 1a) shows large decadal variations, with negative anomalies before 1935, from the mid-1940s to the mid-1960s and after the early 2000s, and positive anomalies around 1940 and from the late 1960s to the early 2000s. The $IOBM_{IV}$-related decadal SST anomalies exhibit a basin-wide warm pattern during the positive phases, with large (weak) anomalies from 5°S to 10°N (10°–20°S, Figure 1b). Such phase changes and spatial patterns are also evident in other SST data and are insensitive to the methods applied to estimate the IV-related component (Figure S3 in Supporting Information S1). Note that the total decadal IOBM variations (black line in Figure 2a) and its internal component $IOBM_{IV}$ (blue line in Figure 2a) diverge substantially since the 1950s, suggesting a large role of external forcing during the last 70 years (Figure 2a). IV dominates the Indian SST variations and contributes more than EX to the decadal trends in Indian SSTs during 1930–1986 (Figure 2b). Furthermore, multidecadal variations in EX contribute a larger warming trend during the recent periods since the 1990s (Figure 2b).

3.2. Origins of the Internal Decadal IOBM

The phase changes of $IOBM_{IV}$ are broadly consistent with those of the internally-generated IPO (IPO_{IV}), except for the positive phase transition around the mid-1960s (Figure 1a). We note that the internally-generated AMO (AMO_{IV}) entered a negative phase around this time (red line in Figure 1a). To examine the relationship between the AMO_{IV} and $IOBM_{IV}$, we analyzed the SST ensemble-mean difference fields between the CESM1 Atlantic pacemaker ensemble simulations and its all-forcing historical simulations to quantify Atlantic internal variations and the Pacific and Indian Ocean responses to the Atlantic internal variations.

Our results show that the Atlantic internal SST variations are dominated by the AMO_{IV} and the Pacific SST response to the Atlantic SST variations shows an IPO-like pattern (Figure S4 in Supporting Information S1). Significant anti-correlation ($r = -0.67$, $p < 0.05$) between the AMO_{IV} and Pacific SST decadal variations exists in the Atlantic pacemaker simulations after removing the EX changes. That is, a warm AMO_{IV} could lead to a cold IPO-like SST pattern in the Pacific Ocean, consistent with previous findings (Meehl et al., 2021; Ruprich-Robert et al., 2017). In the Indian Ocean, there exists a basin-wide SST anomaly pattern generated by Atlantic internal variations (Figure 3b). In general, a North Atlantic warm anomaly leads to a cold anomaly in the tropical central eastern Pacific, but a warm anomaly in the western Pacific and Indian oceans (Figures 3b and S4 in Supporting Information S1), through the atmospheric bridge (Li et al., 2016; McGregor et al., 2014). Furthermore, we also examine the two leading EOFs of the Indian Ocean SST anomaly fields generated by Atlantic internal SST variations (Figure S5 in Supporting Information S1). The first EOF shows a cold (warm) anomaly in the western (eastern) Indian Ocean, whose temporal coefficients are anti-correlated ($r = -0.87$, $p < 0.05$) with those of the positive IPO-like SST pattern in the Pacific generated by the same Atlantic SST forcing, while the second EOF exhibits an IOBM-like SST variations, which is similar to the total Indian SST variations from observations (Figure 3c and Figure S5d in Supporting Information S1), although it is not significantly correlated with the AMO_{IV}. Our results suggest that the AMO_{IV} may play a role in modulating the Indian decadal SST variations, and the AMO's influence may partly come through the Pacific Ocean as the Indian response (i.e., EOF1) and the IPO-like response in the Pacific are highly correlated in the Atlantic pacemaker runs.

Consistent with previous studies (Dong et al., 2016; Han, Meehl et al., 2014), in the Pacific pacemaker simulations, the IPO works to generate in-phase ($r = 0.91$, $p < 0.05$) decadal SST variations in the Indian Ocean (Figure S6 in Supporting Information S1), with the phase transitions around the 1940, 1970 and 1990s. The IPO-like SST

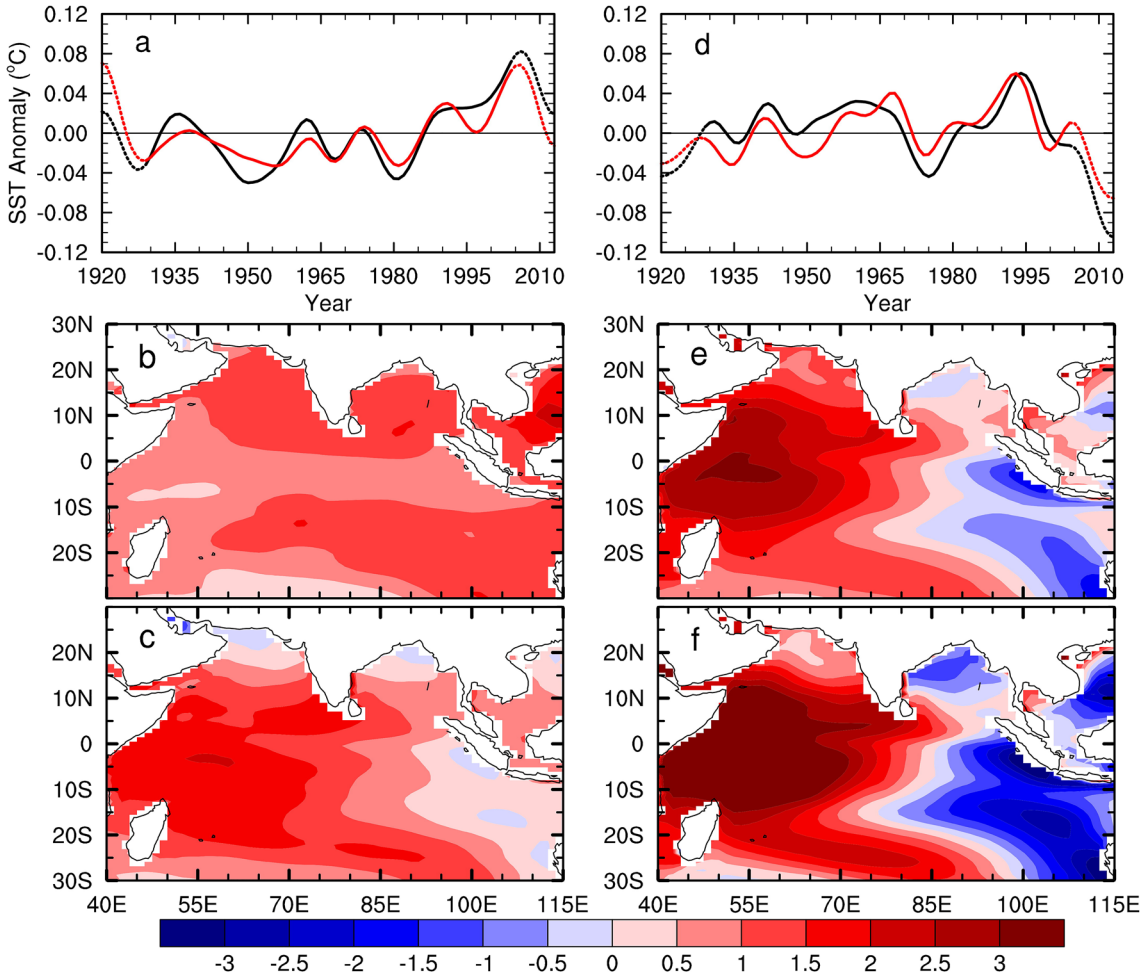

Figure 3. (a) Time series of the smoothed sea surface temperature (SST) anomalies (black line, °C) averaged over the Indian Ocean from the internally-generated Atlantic-induced variations (mostly AMO_{IV}). The red line is the smoothed SST anomalies (i.e., PC2*EOF2, Figures S5c and S5d in Supporting Information S1) in the Indian Ocean. We use the ensemble mean difference between the Community Earth System Model Version 1 (CESM1) 10-member Atlantic pacemaker simulations and 40-member historical all-forcing runs to represent the internally-generated Atlantic-induced variations. (b) The spatial pattern obtained by regressing the smoothed internally-generated Atlantic-induced SST fields from 1920 to 2013 onto the black line in (a). (c) The regressed spatial pattern onto the red line in (a). (d–f) Same as (a–c), but from the internally-generated tropical Eastern Pacific (TEP)-induced variations. We use the ensemble mean difference between the CESM1 20-member Pacific pacemaker simulations and 40-member historical all-forcing runs to represent the TEP-induced internal variations (mostly IPO_{IV}). The red line in (d) is the smoothed SST anomalies (i.e., PC1*EOF1) in the Indian Ocean from the internally-generated TEP-induced variations.

forcing in the tropical Pacific also leads to an in-phase SST response in the tropical Atlantic (i.e., a warm anomaly in the central eastern Pacific leads to a warm anomaly in the tropical Atlantic), consistent with previous findings (Meehl et al., 2021). Note that the simulated IPO_{IV}-induced decadal SST variations in the Indian Ocean show an Indian Ocean dipole (IOD)-like pattern (Figures 3e and 3f). We also examined the IV-induced decadal SST variations in a long preindustrial control run and 40-member all-forcing simulations by the CESM1 (Figures S7 and S8 in Supporting Information S1). The IPO_{IV}-related SST anomalies in the Indian Ocean also show an IOD-like pattern (Figures S7c and S8 in Supporting Information S1). Furthermore, the IOD-like SST biases also exist in some CMIP6 models (Figure S9 in Supporting Information S1). This deficiency may be related to an overestimation of upwelling processes off Sumatra in some climate models, including CESM1 (Cai & Cowan, 2013; Du et al., 2013). Previous studies suggest that the mean depth of the thermocline off Sumatra in climate models is too shallow, inducing a strong cold tongue structure (Zheng et al., 2013). As the CanESM5 model broadly captures the internal IOBM pattern (Figure S9 in Supporting Information S1), we also analyzed the CanESM5 large ensembles for comparison with the results from the CESM1-LE. Overall, the results are similar when using the CanESM5 large ensembles to define the internal and forced Indian decadal variations (Figure S10 in Supporting Information S1).

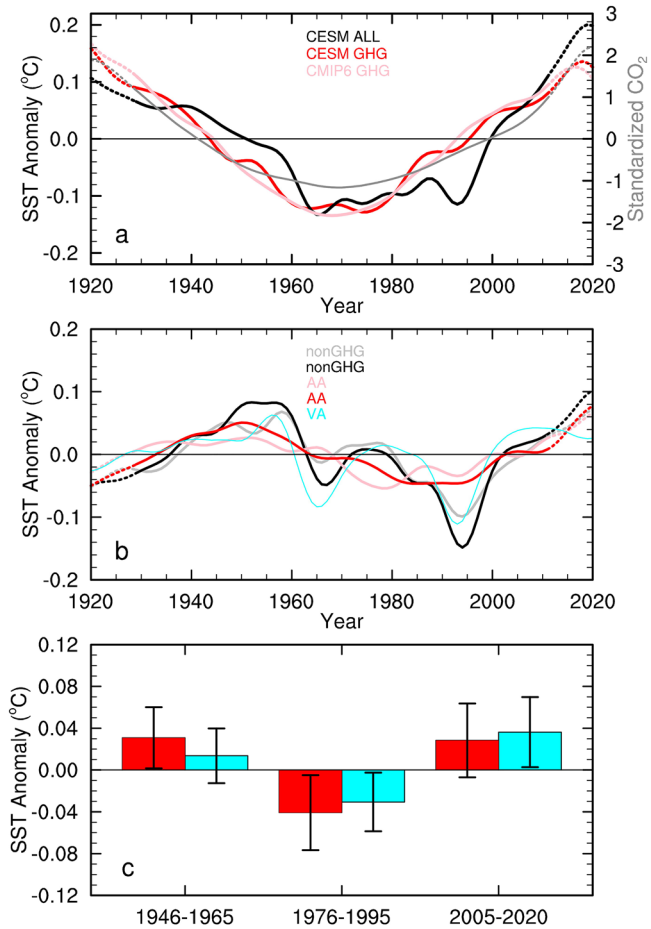

Figure 4. (a) Time series of the linearly detrended and smoothed sea surface temperature (SST) anomalies (°C) from 1920 to 2020 averaged over the Indian Ocean from the ensemble mean of the all-forcing (ALL, black line) and greenhouse gas (GHG)-forcing only (GHG, red line) Community Earth System Model Version 1 (CESM1) simulations. The pink line shows the smoothed and detrended Indian SST anomalies from the Coupled Model Intercomparison Project Phase 6 (CMIP6) multi-model ensemble mean of the GHG-forcing only simulations. Also shown are the normalized time series of linearly detrended (i.e., with the linear trend over 1920–2020 removed) global-mean atmospheric CO_2 concentration from the CESM1 simulations. (b) Time series of the linearly detrended and smoothed SST anomalies (°C, relative to 1920–2020 mean) averaged over the Indian Ocean from the ensemble mean of the CESM1 XGHG (i.e., all forcing, except that GHG forcing agent is held fixed) forcing simulations from 1920–2020 (grey line), the CMIP6 anthropogenic aerosols (AA, red line) and volcanic aerosols (VA, blue line) forcing only simulations from 1920 to 2020. The black line shows the SST anomaly averaged over the Indian Ocean from the CMIP6 ALL forcing minus GHG forcing only simulations, which also represents the non-GHG forced signal. The pink line shows the SST anomaly from the CESM1 ALL minus XAER (i.e., all forcing, except that industrial aerosol forcing agent is held fixed) forcing simulations, which represents the anthropogenic aerosol forced signal. The model simulations were linearly detrended before calculating the anomalies. The data near the two ends are derived with mirrored data in the filtering and thus are less reliable, they are marked by the dashed lines. (c) The epoch-mean of the SST anomalies (°C) averaged over the Indian Ocean during three phase periods from the CMIP6 AA only (red) and VA only (blue) simulations. The error bars denote the ±1 standard deviation range of the inter-model variations.

To find out to what extent the observed Indian decadal SST variations are forced by the remote influences from the Pacific and Atlantic Oceans, we further examine the SST changes between the warm and cold phases of the $IOBM_{IV}$. As the $IOBM_{IV}$ is broadly in-phase (out-of-phase) with IPO (AMO) since 1970s (Figure 1a), we focus on the period between 2005 and 2013 (an $IOBM_{IV}$ cold phase) and 1976–1995 (an $IOBM_{IV}$ warm phase). In the observations, the $IOBM_{IV}$-related SST variations exhibit a decadal cooling from 1976 to 1995 to 2005–2013, with a cooling trend from 1987 to 2013 (Figure S11 in Supporting Information S1). The influence of the IPO on the decadal IOBM is opposite to that of the AMO, and these two modes show similar magnitudes. The sum of these two components reflects an estimate of the IV in observations due to tropical Pacific and North Atlantic SST variations, although this linear summation does not take into account inter-basin interactions (Cai et al., 2019). The residual was mainly considered as the local variability and other remote influence. Furthermore, we also used the EM difference between the CESM1 Indian pacemaker simulations and all-forcing historical runs by CESM1 to represent the total internal Indian Ocean variations (Figure S11 in Supporting Information S1), which ideally should match the total internal variations from observations (i.e., IV component). However, there exist biases between the observations-based method and pacemaker framework. The $IOBM_{IV}$-related SST variations (Figure 3c) in response to Atlantic internal SST forcing (i.e., AMO_{IV}) contribute to the decadal warming. Note that the IPO and AMO may not be independent from each other (d'Orgeville & Peltier, 2007; Kucharski et al., 2016; Nigam et al., 2020; Zhang & Delworth, 2007). There exist two-way connections between the Pacific and Atlantic Oceans both in observations and models (Cai et al., 2019; Meehl et al., 2021; Wang, 2019).

3.3. Impacts of External Forcing

Decadal changes in external forcing, such as GHGs and aerosols, cause the IOBM (black line in Figure 2) to stay in a cold phase until the early 1980s, while the $IOBM_{IV}$ already entered a warm phase around 1965 (Figure 2a). Since the early 2000s, external forcing keeps the IOBM in a warm phase while its internal component enters a new cold phase (Figure 2a). We further examine individual external forcing agents (e.g., GHG and aerosols) that may contribute to Indian decadal variations. Note that we linearly detrended the EX changes in order to focus on the forced nonlinear component. Thus, the forced decadal to multidecadal variations examined here do not include the changes associated with the long-term liner trend. GHG-forced Indian decadal SST variations (with its linear trend over 1920–2020 removed) show a downward trend from 1920 to 1965 and an upward trend since the late 1970s, contributing to the upward trend for the IOBM since the late 1970s (Figure 4a). GHG-forced SST variations show mostly in phase variations with the EX component in Indian SSTs since 1920 (Figure 4a) and the phase change during the 1940s in the GHG-induced SST anomalies is also roughly consistent with $IOBM_{IV}$'s phase change during that period (Figures 2a and 4a). Thus, the linearly-detrended GHG-forced variations enhance (suppress) the total Indian SST decadal anomalies before the mid-1940s and after the mid-1990s (between them) (Figure 4a).

In addition to GHGs, non-GHG forcing also contribute to the Indian SST variations. Volcanic aerosols caused strong decadal cold anomaly in the Indian Ocean from 1963 to 1966 and from 1991 to 1994 due to the 1963 Mount Agung and 1991 Pinatubo eruptions (Maher et al., 2015), while

linearly-detrended anthropogenic aerosol anomalies (similar to an AMO-like oscillation, Qin et al., 2020a) led to steady cooling from ~ 1965 to 2000 (Figure 4b). Such cooling kept the IOBM at a low level until the 1970s, while its internal component rose steadily since ~1951 (Figure 2a). For the period since the early 2000s, the decadal aerosol forcing led to Indian warming and thus contributed to the recent IOBM warm anomalies (Figures 4b and 4c). Both volcanic and anthropogenic aerosols contributed roughly equally to the non-GHG forced Indian SST variations since the 1970s. Furthermore, decadal changes in non-GHG forcing are roughly out-of-phase with the $IOBM_{IV}$ since the 1950s (Figures 2a and 4b and 4c).

4. Conclusions and Discussion

To quantify the roles of external forcing and internal climate variability in Indian Ocean decadal SST variations (with a focus on the decadal IOBM), we analyzed observations and model simulations from CMIP6 and CESM1 since 1920. We found that the internally-generated decadal IOBM variations from 1920 to 2020 may arise from remote influences from the tropical Pacific and North Atlantic Oceans and possible contributions from the local dynamics of the Indian Ocean, rather than being driven primarily by the tropical Pacific SST variations (i.e., IPO) as previously thought (Dong e al., 2016; Han, Meehl et al., 2014). The internally-generated decadal IOBM, IPO and AMO exhibit strong correlations, although the AMO may have an opposite effect. Our results also suggest that the decadal variations in GHGs and aerosols have dampened the internally-induced decadal IOBM variations since the 1950s. Therefore, both external forcing and internal variability have contributed to the observed decadal IOBM variations, especially since the 1950s.

In this study, we assumed that the unforced internal variability (including any internal decadal variations) comes from the tropical Pacific and North Atlantic oceans and possible contributions from the local dynamics of the Indian Ocean. However, remote influences from other regions may also play a role (Krishnamurthy & Krishnamurthy, 2016). For example, the Southern Ocean (Zhang et al., 2021), South Atlantic (Xue et al., 2018), extratropical Pacific (Krishnamurthy & Krishnamurthy, 2016), and the North Atlantic Oscillation (Xie et al., 2021) may contribute to the Indian Ocean multidecadal variability. We also notice that current climate models (e.g., CESM1) tend to overestimate the magnitude of the SST variability in the southeastern Indian Ocean, which implies that the models may not realistically simulate the decadal to multidecadal variations (Kravtsov et al., 2018; Mann et al., 2020) or inter-basin teleconnection (Cai et al., 2019; Li et al., 2016) for the Indian Ocean. The CESM1 Indian Ocean pacemaker simulation fails to follow the observed decadal IOBM well since the 1980s, leading to underestimate (overestimate) the observed amplitudes from the 1980s to the 1990s (since the late 1990s) (Figure S12 in Supporting Information S1). Therefore, the modeled IOBM results in smaller 2005–2013 minus 1976–1995 decadal differences (Figure S11 in Supporting Information S1). We also further separated the Indian basin into the western and eastern parts in order to avoid cancellation of the IOD-like biases. The estimated decadal SST variations over the western Indian Ocean forced by the tropical Pacific are more than twice as large as the decadal IOBM (Figures S11 and S13 in Supporting Information S1). Thus, the simulated IPO-induced decadal IOBM variations could be underestimated, as the IOBM can be contaminated by its IPO-induced variations (Figures S11 and S13 in Supporting Information S1). For the SST variations induced by the North Atlantic Ocean, the magnitude is similar when using the whole Indian Ocean or western part to define the IOBM, although the AMO's influence may partly come through the Pacific Ocean. Overall, our further analyses suggest that the CESM1 model cannot reproduce the internal decadal SST variations since the 1980s and decadal dominance of the IOD mainly influences Indian SST responses to tropical Pacific SST forcing. These two issues may underestimate the contributions of local variability and tropical Pacific SST forcing to the recent decadal IOBM since the 1980s. Note that the IOD-like SST biases may have an impact on Pacific SST variations (Cai et al., 2019). For example, there exists interactive feedback between the IOD and El Niño/Southern Oscillation on interannual time scales (Izumo et al., 2010; Kug & Kang, 2006). Further efforts to reduce the common model biases could help advance our understanding of Indian Ocean decadal variability.

Data Availability Statement

HadISST data were downloaded from https://www.metoffice.gov.uk/hadobs/hadisst/. The CESM1 large ensemble simulations are available online at https://www.earthsystemgrid.org/dataset/ucar.cgd.ccsm4.cesmLE.html. Datasets from CMIP6 simulations were archived at https://esgf-node.llnl.gov/search/cmip6/. The CMIP6 models used in this study are listed in Table S1 of Supporting Information S1.

Acknowledgments
This work was supported by the National Natural Science Foundation of China (42088101, 42075022) and the National Natural Science Foundation of Jiangsu Province (BK20200096). A. Dai was supported by the National Science Foundation (grant nos. AGS-2015780 and OISE-1743738). We acknowledge the CESM Large Ensemble Community Project and supercomputing resources provided by NSF/CISL/Yellowstone. We also acknowledge the World Climate Research Programme, which, through its Working Group on Coupled Modelling, coordinated and promoted CMIP6. We thank the climate modeling groups for producing and making available their model output, the Earth System Grid Federation (ESGF) for archiving the data and providing access, and the multiple funding agencies who support CMIP6 and ESGF. The authors acknowledge the editor and two anonymous reviewers for their constructive comments, which help greatly improve this manuscript.

References

Cai, W., & Cowan, T. (2013). Why is the amplitude of the Indian Ocean dipole overly large in CMIP3 and CMIP5 climate models? *Geophysical Research Letters*, *40*(6), 1200–1205. https://doi.org/10.1002/grl.50208

Cai, W., Wu, L., Lengaigne, M., Li, T., McGregor, S., Kug, J. S., et al. (2019). Pantropical climate interactions. *Science*, *363*(6430), eaav4236. https://doi.org/10.1126/science.aav4236

Dai, A., & Bloecker, C. E. (2019). Impacts of internal variability on temperature and precipitation trends in large ensemble simulations by two climate models. *Climate Dynamics*, *52*(1–2), 289–306. https://doi.org/10.1007/s00382-018-4132-4

Dai, A., Fyfe, J. C., Xie, S.-P., & Dai, X. (2015). Decadal modulation of global surface temperature by internal climate variability. *Nature Climate Change*, *5*(6), 555–559. https://doi.org/10.1038/nclimate2605

Davis, R. E. (1976). Predictability of sea surface temperature and sea level pressure anomalies over the North Pacific Ocean. *Journal of Physical Oceanography*, *6*, 2492–3266. https://doi.org/10.1175/1520-0485(1978)008<0233:POSLPA>2.0.CO;2

Deser, C., Guo, R., & Lehner, F. (2017). The relative contributions of tropical Pacific sea surface temperatures and atmospheric internal variability to the recent global warming hiatus. *Geophysical Research Letters*, *44*(15), 7945–7954. https://doi.org/10.1002/2017GL074273

Deser, C., Phillips, A. S., & Alexander, M. A. (2010). Twentieth century tropical sea surface temperature trends revisited. *Geophysical Research Letters*, *37*(10), L10701. https://doi.org/10.1029/2010GL043321

Deser, C., Phillips, A. S., Simpson, I. R., Rosenbloom, N., Coleman, D., Lehner, F., et al. (2020). Isolating the evolving contributions of anthropogenic aerosols and greenhouse gases: A new CESM1 large ensemble community resource. *Journal of Climate*, *33*(18), 7835–7858. https://doi.org/10.1175/JCLI-D-20-0123.1

Dong, L., & McPhaden, M. J. (2017). Why has the relationship between Indian and Pacific Ocean decadal variability changed in recent decades? *Journal of Climate*, *30*(6), 1971–1983. https://doi.org/10.1175/JCLI-D-16-0313.1

Dong, L., Zhou, T., Dai, A., Song, F., Wu, B., & Chen, X. (2016). The footprint of the inter-decadal Pacific oscillation in Indian Ocean sea surface temperatures. *Scientific Reports*, *6*(1), 21251. https://doi.org/10.1038/srep21251

d'Orgeville, M., & Peltier, W. R. (2007). On the Pacific decadal oscillation and the Atlantic multidecadal oscillation: Might they be related? *Geophysical Research Letters*, *34*(23), L23705. https://doi.org/10.1029/2007GL031584

Du, Y., Xie, S.-P., Yang, Y.-L., Zheng, X.-T., Liu, L., & Huang, G. (2013). Indian Ocean variability in the CMIP5 multimodel ensemble: The basin mode. *Journal of Climate*, *26*(18), 7240–7266. https://doi.org/10.1175/JCLI-D-12-00678.1

Eyring, V., Bony, S., Meehl, G. A., Senior, C. A., Stevens, B., Stouffer, R. J., & Taylor, K. E. (2016). Overview of the Coupled Model Intercomparison Project Phase 6 (CMIP6) experimental design and organization. *Geoscientific Model Development*, *9*(5), 1937–1958. https://doi.org/10.5194/gmd-9-1937-2016

Han, W., Meehl, G. A., Hu, A., Alexander, M. A., Yamagata, T., Yuan, D., et al. (2014). Intensification of decadal and multi-decadal sea level variability in the Western tropical Pacific during recent decades. *Climate Dynamics*, *43*(5–6), 1357–1379. https://doi.org/10.1007/s00382-013-1951-1

Han, W., Vialard, J., McPhaden, M. J., Lee, T., Masumoto, Y., Feng, M., & de Ruijter, W. P. M. (2014). Indian Ocean decadal variability: A review. *Bulletin of the American Meteorological Society*, *95*(11), 1679–1703. https://doi.org/10.1175/BAMS-D-13-00028.1

Henley, B. J., Gergis, J., Karoly, D. J., Power, S., Kennedy, J., & Folland, C. K. (2015). A tripole index for the Interdecadal Pacific Oscillation. *Climate Dynamics*, *45*(11–12), 3077–3090. https://doi.org/10.1007/s00382-015-2525-1

Hua, W., Dai, A., & Qin, M. (2018). Contributions of internal variability and external forcing to the recent Pacific decadal variations. *Geophysical Research Letters*, *45*(14), 7084–7092. https://doi.org/10.1029/2018GL079033

Hua, W., Dai, A., Zhou, L., Qin, M., & Chen, H. (2019). An externally-forced decadal rainfall seesaw pattern over the Sahel and southeast Amazon. *Geophysical Research Letters*, *46*(2), 923–932. https://doi.org/10.1029/2018GL081406

Hua, W., Qin, M., Dai, A., Zhou, L., Chen, H., & Zhang, W. (2021). Reconciling human and natural drivers of the tripole pattern of multidecadal summer temperature variations over Eurasia. *Geophysical Research Letters*, *48*(14), e2021GL093971. https://doi.org/10.1029/2021GL093971

Izumo, T., Vialard, J., Lengaigne, M., de Boyer Montegut, C., Behera, S. K., Luo, J. J., et al. (2010). Influence of the state of the Indian Ocean dipole on the following year's El Niño. *Nature Geoscience*, *3*, 168–172. https://doi.org/10.1038/ngeo760

Kay, J. E., Deser, C., Phillips, A. S., Mai, A., Hannay, C., Strand, G., et al. (2015). The Community Earth System Model (CESM) large ensemble project: A community resource for studying climate change in the presence of internal climate variability. *Bulletin of the American Meteorological Society*, *96*(8), 1333–1349. https://doi.org/10.1175/BAMS-D-13-00255.1

Kravtsov, S., Grimm, C., & Gu, S. (2018). Global-scale multidecadal variability missing in state-of-the-art climate models. *npj Climate and Atmospheric Science*, *1*, 34. https://doi.org/10.1038/s41612-018-0044-6

Krishnamurthy, L., & Krishnamurthy, V. (2016). Decadal and interannual variability of the Indian Ocean SST. *Climate Dynamics*, *46*(1–2), 57–70. https://doi.org/10.1007/s00382-015-2568-3

Kucharski, F., Ikram, F., Molteni, F., Farneti, R., Kang, I. S., No, H. H., et al. (2016). Atlantic forcing of Pacific decadal variability. *Climate Dynamics*, *46*(7–8), 2337–2351. https://doi.org/10.1007/s00382-015-2705-z

Kug, J.-S., & Kang, I.-S. (2006). Interactive feedback between ENSO and the Indian Ocean. *Journal of Climate*, *19*(9), 1784–1801. https://doi.org/10.1175/JCLI3660.1

Li, X., Xie, S.-P., Gille, S. T., & Yoo, C. (2016). Atlantic-induced pan-tropical climate change over the past three decades. *Nature Climate Change*, *6*(3), 275–279. https://doi.org/10.1038/nclimate2840

Luo, J.-J., Sasakia, W., & Masumoto, Y. (2012). Indian Ocean warming modulates Pacific climate change. *Proceedings of the National Academy of Sciences of the United States of America*, *109*(46), 18701–18706. https://doi.org/10.1073/pnas.1210239109

Maher, N., McGregor, S., England, M. H., & Gupta, A. S. (2015). Effects of volcanism on tropical variability. *Geophysical Research Letters*, *42*(14), 6024–6033. https://doi.org/10.1002/2015GL064751

Mann, M. E., Steinman, B. A., & Miller, S. K. (2020). Absence of internal multidecadal and interdecadal oscillations in climate model simulations. *Nature Communications*, *11*(1), 49. https://doi.org/10.1038/s41467-019-13823-w

McGregor, S., Timmermann, A., Stuecker, M. F., England, M. H., Merrifield, M., Jin, F.-F., & Chikamoto, Y. (2014). Recent Walker circulation strengthening and Pacific cooling amplified by Atlantic warming. *Nature Climate Change*, *4*(10), 888–892. https://doi.org/10.1038/nclimate2330

Meehl, G. A., Hu, A., Castruccio, F., England, M. H., Bates, S. C., Danabasoglu, G., et al. (2021). Atlantic and Pacific tropics connected by mutually interactive decadal-timescale processes. *Nature Geoscience*, *14*(1), 36–42. https://doi.org/10.1038/s41561-020-00669-x

Nigam, S., Sengupta, A., & Ruiz-Barradas, A. (2020). Atlantic–Pacific links in observed multidecadal SST variability: Is the Atlantic multidecadal oscillation's phase reversal orchestrated by the Pacific decadal oscillation? *Journal of Climate*, *33*(13), 5479–5505. https://doi.org/10.1175/JCLI-D-19-0880.1

Qin, M., Dai, A., & Hua, W. (2020a). Aerosol-forced multidecadal variations across all ocean basins in models and observations since 1920. *Science Advances*, *6*(29), eabb0425. https://doi.org/10.1126/sciadv.abb0425

Qin, M., Dai, A., & Hua, W. (2020b). Quantifying contributions of internal variability and external forcing to Atlantic multidecadal variability since 1870. *Geophysical Research Letters*, *47*(22), e2020GL089504. https://doi.org/10.1029/2020GL089504

Qin, M., Dai, A., & Hua, W. (2022). Influence of anthropogenic warming on the Atlantic multidecadal variability and its impact on global climate in the twenty-first century in the MPI-GE simulations. *Journal of Climate*, *35*(9), 2805–2821. https://doi.org/10.1175/JCLI-D-21-0535.1

Rayner, N. A., Parker, D. E., Horton, E. B., Folland, C. K., Alexander, L. V., & Rowell, D. P. (2003). Global analyses of sea surface temperature, sea ice, and night marine air temperature since the late nineteenth century. *Journal of Geophysical Research*, *108*(D14), 4407. https://doi.org/10.1029/2002JD002670

Ruprich-Robert, Y., Msadek, R., Castruccio, F., Yeager, S., Delworth, T., & Danabasoglu, G. (2017). Assessing the climate impacts of the observed Atlantic multidecadal variability using the GFDL CM2.1 and NCAR CESM1 global coupled models. *Journal of Climate*, *30*(8), 2785–2810. https://doi.org/10.1175/JCLI-D-16-0127.1

Steinman, B. A., Mann, M. E., & Miller, S. K. (2015). Atlantic and Pacific multidecadal oscillations and Northern Hemisphere temperatures. *Science*, *347*(6225), 988–991. https://doi.org/10.1126/science.1257856

Wang, C. (2019). Three-ocean interactions and climate variability: A review and perspective. *Climate Dynamics*, *53*(7–8), 5119–5136. https://doi.org/10.1007/s00382-019-04930-x

Xie, S.-P., Hu, K., Hafner, J., Tokinaga, H., Du, Y., Huang, G., & Sampe, T. (2009). Indian Ocean capacitor effect on Indo-Western Pacific climate during the summer following El Niño. *Journal of Climate*, *22*(3), 730–747. https://doi.org/10.1175/2008JCLI2544.1

Xie, T., Li, J., Chen, K., Zhang, Y., & Sun, C. (2021). Origin of Indian Ocean multidecadal climate variability: Role of the North Atlantic Oscillation. *Climate Dynamics*, *56*(9–10), 3277–3294. https://doi.org/10.1007/s00382-021-05643-w

Xue, J., Sun, C., Li, J., & Mao, J. (2018). South Atlantic forced multidecadal teleconnection to the midlatitude south Indian Ocean. *Geophysical Research Letters*, *45*(16), 8480–8489. https://doi.org/10.1029/2018GL078990

Yang, D., Arblaster, J. M., Meehl, G. A., England, M. H., Lim, E.-P., Bates, S., & Rosenbloom, N. (2020). Role of tropical variability in driving decadal shifts in the Southern Hemisphere summertime eddy-driven jet. *Journal of Climate*, *33*(13), 5445–5463. https://doi.org/10.1175/JCLI-D-19-0604.1

Zhang, L., Han, W., Karnauskas, K. B., Meehl, G. A., Hu, A., Rosenbloom, N., & Shinoda, T. (2019). Indian Ocean warming trend reduces Pacific warming response to anthropogenic greenhouse gases: An interbasin thermostat mechanism. *Geophysical Research Letters*, *46*(19), 10882–10890. https://doi.org/10.1029/2019GL084088

Zhang, L., Han, W., & Sienz, F. (2018). Unraveling causes for the changing behavior of the tropical Indian Ocean in the past few decades. *Journal of Climate*, *31*(6), 2377–2388. https://doi.org/10.1175/JCLI-D-17-0445.1

Zhang, R., & Delworth, T. L. (2007). Impact of the Atlantic multidecadal oscillation on North Pacific climate variability. *Geophysical Research Letters*, *34*(23), L23708. https://doi.org/10.1029/2007GL031601

Zhang, X., Deser, C., & Sun, L. (2021). Is there a tropical response to recent observed Southern Ocean cooling? *Geophysical Research Letters*, *48*(5), e2020GL091235. https://doi.org/10.1029/2020GL091235

Zheng, X.-T., Xie, S.-P., Du, Y., Liu, L., Huang, G., & Liu, Q. (2013). Indian Ocean dipole response to global warming in the CMIP5 multimodel ensemble. *Journal of Climate*, *26*(16), 6067–6080. https://doi.org/10.1175/JCLI-D-12-00638.1

References From the Supporting Information

Deser, C., Alexander, M. A., Xie, S.-P., & Phillips, A. S. (2010). Sea surface temperature variability: Patterns and mechanisms. *Annual Review of Marine Science*, *2*(1), 115–143. https://doi.org/10.1146/annurev-marine-120408-151453

Huang, B., Thorne, P. W., Banzon, V. F., Boyer, T., Chepurin, G., Lawrimore, J. H., et al. (2017). Extended reconstructed sea surface temperature version 5 (ERSSTv5), upgrades, validations, and intercomparisons. *Journal of Climate*, *30*(20), 8179–8205. https://doi.org/10.1175/JCLI-D-16-0836.1

Ishii, M., Shouji, A., Sugimoto, S., & Matsumoto, T. (2005). Objective analyses of sea-surface temperature and marine meteorological variables for the 20th century using ICOADS and the Kobe Collection. *International Journal of Climatology*, *25*(7), 865–879. https://doi.org/10.1002/joc.1169

Kaplan, A., Cane, M. A., Kushnir, Y., Clement, A. C., Blumenthal, M. B., & Rajagopalan, B. (1998). Analyses of global sea surface temperature 1856-1991. *Journal of Geophysical Research*, *103*(C9), 18567–18589. https://doi.org/10.1029/97JC01736